

Figure 19: The phase diagram for system (32) at the cubic nonlinearity parameter $\gamma = 1$. The thick red and magenta curves bound the region spanned by solid ellipses where an asymptotically stable periodic solution to ODE (46) exists. The medium-weight solid curves of blue and green shades depict the level sets of $|v|^2 > 1$ corresponding to asymptotically stable periodic solutions. The black slanted lines $\tilde{\sigma} - \tilde{\mu} = \pm 1$ correspond to stable periodic solutions with $|v|^2 = 1$. The medium-weight solid and thin dashed curves of dark red and dark yellow shades correspond, respectively, to asymptotically stable and unstable periodic solutions with $\frac{1}{2} < |v|^2 < 1$. The dashed curves of grey tones depict ellipses with $0 < |v|^2 < \frac{1}{2}$. The black numbers next to the curves indicate the corresponding values of $|v|^2$.

chosen bifurcation parameter to achieve it. In other words, if the number of the additional parameters is equal to the codimension of the tangent space of the normal form. The third step is to identify the loci of singularities, i.e., parameter values, at which the bifurcation diagram undergoes a qualitative change.

Eq. (59) is cubic in x . Cubic equations admit two types of singularities, *hysteresis* and *bifurcation*, illustrated in Fig. 20. The loci of singularities partition the parameter space into regions in each of which the bifurcation diagram remains qualitatively the same. Therefore, it suffices to plot one representative bifurcation diagram for each region of the unfolding parameter space, partitioned by the singularity hypersurfaces.

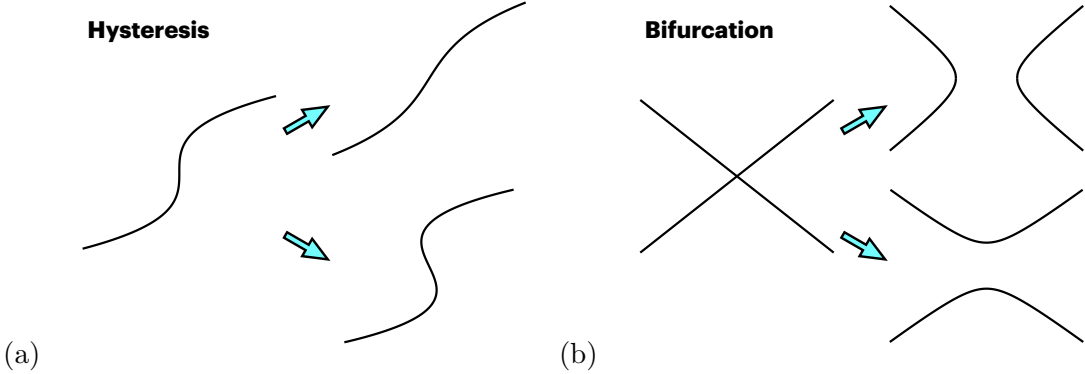


Figure 20: Nonpersistent diagrams of hysteresis and bifurcation types. (a): A bifurcation diagram of hysteresis type on the left transforms into a branch with a unique solution on the top right, or with a three-solution interval on the bottom right, as a result of an arbitrarily small perturbation. (b): A bifurcation diagram of bifurcation type on the left transforms into one of the diagrams on the right, as a result of an arbitrarily small perturbation.

Examining Eq. (59), we choose σ as a bifurcation parameter and observe that it can be viewed as an unfolding of the following \mathbb{Z}_2 -symmetric normal form (see Table 5.1 on page 263 in Section VI.5 in [36]):

$$g(x, \sigma) := x^3 + \sigma^2 x. \quad (60)$$

Its \mathbb{Z}_2 -codimension is 1, while its full co-dimension is 5. Eq. (59) has four additional parameters, μ , ε , λ , and γ . The parameter μ is the excitation parameter of the first cell in Eq. (46). It is positive by assumption. It can be eliminated by redefining λ as $\lambda\sqrt{\mu}$ and ε as $\mu + \varepsilon$. We choose not to do it. Instead, we fix its value and treat it as a constant.

Thus, Eq. (59) can be viewed as a three-parameter unfolding of Eq. (60). It is neither a \mathbb{Z}_2 -unfolding, nor the full universal unfolding of $g(x, \sigma)$. Next, we proceed to finding the loci of nonpersistent phenomena: hysteresis, \mathcal{H} , and bifurcation, \mathcal{B} , singularities. The conditions for these singularities are specified in Definition 5.1 in Section III.5 in [36].

The conditions for the hysteresis singularity are $G = G_x = G_{xx} = 0$. This gives the following system:

$$G = x^3(1 + \gamma^2) - 2(\mu + \varepsilon + \sigma\gamma)x^2 + [(\mu + \varepsilon)^2 + \sigma^2]x - \lambda^2\mu = 0 \quad (61a)$$

$$G_x = 3x^2(1 + \gamma^2) - 4(\mu + \varepsilon + \sigma\gamma)x + (\mu + \varepsilon)^2 + \sigma^2 = 0 \quad (61b)$$

$$G_{xx} = 6x(1 + \gamma^2) - 4(\mu + \varepsilon + \sigma\gamma) = 0. \quad (61c)$$

System (61a), (61b), (61c) can be solved for ε , σ , and $|u|^2 \equiv x$ in terms of λ , μ , and γ , defining the hysteresis set as (see Appendix C):

$$\mathcal{H} = \left\{ \varepsilon = \frac{3}{2} \frac{1 \pm \frac{1}{\sqrt{3}}\gamma}{(1 + \gamma^2)^{1/3}} \lambda^{2/3} \mu^{1/3} - \mu, \quad \sigma = \frac{3}{2} \frac{\gamma \mp \frac{1}{\sqrt{3}}}{(1 + \gamma^2)^{1/3}} \lambda^{2/3} \mu^{1/3}, \quad |u|^2 = \frac{\lambda^{2/3} \mu^{1/3}}{(1 + \gamma^2)^{1/3}} \right\}. \quad (62)$$

The bifurcation conditions are $G = G_x = G_\sigma = 0$, i.e.,

$$G = x^3(1 + \gamma^2) - 2(\mu + \varepsilon + \sigma\gamma)x^2 + [(\mu + \varepsilon)^2 + \sigma^2]x - \lambda^2\mu = 0 \quad (63a)$$

$$G_x = 3x^2(1 + \gamma^2) - 4(\mu + \varepsilon + \sigma\gamma)x + (\mu + \varepsilon)^2 + \sigma^2 = 0 \quad (63b)$$

$$G_\sigma = -2\gamma x^2 + 2\sigma x = 0. \quad (63c)$$

From Eq. (63c), we find $\gamma = \sigma/x$. Plugging it into Eq. (63b) yields

$$(x - (\mu + \varepsilon))(3x - (\mu + \varepsilon)) = 0, \quad \text{i.e.} \quad x = \mu + \varepsilon \quad \text{or} \quad 3x = \mu + \varepsilon. \quad (64)$$

The conditions $x = \mu + \varepsilon$, $\gamma = \sigma/x$ and Eq. (63a) yield $\lambda^2\mu = 0$, which implies $\lambda = 0$, since we have assumed that $\mu > 0$. The conditions $3x = \mu + \varepsilon$, $\gamma = \sigma/x$ and Eq. (63a) yield $4x^3 = \lambda^2\mu$. Therefore, the bifurcation set is

$$\mathcal{B} = \begin{cases} \lambda = 0, & \sigma = \gamma(\mu + \varepsilon), \quad |u|^2 = \mu + \varepsilon, \\ \frac{4}{27}(\mu + \varepsilon)^3 = \lambda^2\mu, & \sigma = \gamma \frac{\mu + \varepsilon}{3}, \quad |u|^2 = \frac{\mu + \varepsilon}{3}. \end{cases} \quad (65)$$

Eqs. (62) and (65) defining the hysteresis, \mathcal{H} , and bifurcation, \mathcal{B} , sets allow us to plot slices of \mathcal{H} and \mathcal{B} in the (ε, λ) -plane at any given γ . Fig. 21 displays these slices at $\mu = 0.2$ and $\gamma \in \{0, \frac{1}{3}, 1.5, 10\}$.

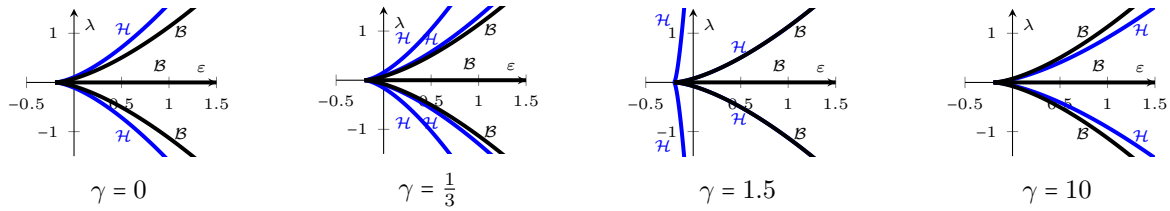


Figure 21: The hysteresis, \mathcal{H} , and bifurcation, \mathcal{B} sets for Eq. (59) at $\mu = 0.2$ and selected values of γ .

Fig. 21 and Eqs. (62) and (65) suggest the following observations:

- The slice structure is symmetric with respect to the map $(\sigma, \gamma) \mapsto (-\sigma, -\gamma)$ and $\lambda \mapsto -\lambda$.
- The \mathcal{B} -slices are independent of γ .
- At $\gamma = 0$, the two \mathcal{H} -slices in the upper half-plane $\lambda > 0$ coincide.
- As $\gamma \rightarrow \sqrt{3}$, the \mathcal{H} -slices with the “+” sign in front of $\frac{1}{\sqrt{3}}\gamma$ approach the \mathcal{B} -slices:

$$\lambda = \pm \left(\frac{2(\mu + \varepsilon)}{3 \left[1 + \frac{1}{\sqrt{3}}\gamma \right]} \right)^{3/2} \left(\frac{1 + \gamma^2}{\mu} \right)^{1/2} \rightarrow \pm \frac{2(\mu + \varepsilon)^{3/2}}{(27\mu)^{1/2}}. \quad (66)$$

On the other hand, the \mathcal{H} -slices with the “-” sign in front of $\frac{1}{\sqrt{3}}\gamma$,

$$\lambda = \pm \left(\frac{2(\mu + \varepsilon)}{3 \left[1 - \frac{1}{\sqrt{3}}\gamma \right]} \right)^{3/2} \left(\frac{1 + \gamma^2}{\mu} \right)^{1/2}, \quad (67)$$

approach vertical line $\epsilon = -\mu$ as $\gamma \rightarrow \sqrt{3}$.

- At $\gamma > \sqrt{3}$, only the \mathcal{H} -slices with the “+” sign in front of $\frac{1}{\sqrt{3}}\gamma$ remain, while the \mathcal{H} -slices with the “-” sign in front of $\frac{1}{\sqrt{3}}\gamma$ disappear.